Development 133, 957-966 doi:10.1242/dev.02266

The *Drosophila* formin DAAM regulates the tracheal cuticle pattern through organizing the actin cytoskeleton

Tamás Matusek[1], Alexandre Djiane[2], Ferenc Jankovics[3], Damian Brunner[3], Marek Mlodzik[2,*] and József Mihály[1,*]

Formins are involved in a wide range of cellular processes that require the remodeling of the actin cytoskeleton. Here, we have analyzed a novel *Drosophila* formin, belonging to the recently described DAAM subfamily. In contrast to previous assumptions, we show that *DAAM* plays no essential role in planar cell polarity signaling, but it has striking requirements in organizing apical actin cables that define the taenidial fold pattern of the tracheal cuticle. These observations provide evidence the first time that the function of the taenidial organization is to prevent the collapse of the tracheal tubes. Our results indicate that although *DAAM* is regulated by *RhoA*, it functions upstream or parallel to the non-receptor tyrosine kinases *Src42A* and *Tec29* to organize the actin cytoskeleton and to determine the cuticle pattern of the *Drosophila* respiratory system.

KEY WORDS: Formin, DAAM, Actin cytoskeleton, Tracheal cuticle, Src kinases, *Drosophila*

INTRODUCTION

Proteins of the formin family play key roles in the regulation of the cytoskeleton. Although the connection between formins and microtubules is less well understood, formins are implicated in a large number of actin-based processes, including cell polarization, division, movement, stress fiber formation and vesicular trafficking (reviewed by Evangelista et al., 2003; Wallar and Alberts, 2003). Recent work suggested that formins catalyze the assembly of unbranched actin structures and nucleate actin filaments directly (Evangelista et al., 1997; Evangelista et al., 2002; Pruyne et al., 2002; Sagot et al., 2002a; Sagot et al., 2002b).

Although all members of this highly conserved family are defined by the presence of the formin homology domain 2 (FH2), which is both necessary and sufficient to nucleate actin in vitro (Pring et al., 2003; Pruyne et al., 2002; Sagot et al., 2002b), formins are multi-domain proteins that contain several other conserved sequences as well. The FH2 domain is usually flanked on the N-terminal side by a proline-rich FH1 domain that can serve as a docking site for the G-actin-binding protein profilin (Chang et al., 1997; Evangelista et al., 1997; Imamura et al., 1997; Watanabe et al., 1997). In addition, the FH1 domain also binds WW domains and SH3 domains, including those of the Src family (Chan et al., 1996; Kamei et al., 1998; Tominaga et al., 2000; Vallen et al., 2000). A distinct formin subfamily, the DRF group (Diaphanous related formins) has the ability to interact with an activated Rho GTPase through an N-terminal GTPase-binding domain (GBD) (Evangelista et al., 1997; Imamura et al., 1997; Kohno et al., 1996; Watanabe et al., 1997). This binding alleviates the autoinhibitory interaction between the GBD and the short C-terminal DAD domain (Diaphanous autoregulatory domain) (Alberts, 2001). Crystallographic analysis of the N-terminal part of mouse Dia1 provided a structural basis of this regulation and identified several other functional domains within this part of the protein, including a dimerization domain (DD), (Fig. 1B) (Otomo et al., 2005a; Rose et al., 2005). In addition, the crystal structure of C-terminal formin domains reveals that the FH2 domain also forms a dimer required for actin nucleation and processive filament capping (Otomo et al., 2005b; Shimada et al., 2004; Xu et al., 2004), strongly suggesting that native formins act in dimeric forms.

Recently, a novel formin subtype, DAAM (Dishevelled-associated activator of morphogenesis), has been identified and implicated in planar cell polarity signaling during *Xenopus* gastrulation (Habas et al., 2001). The polarized orientation of cells within the plane of a tissue, or planar cell polarization (PCP), is an important aspect of cellular differentiation and is often necessary to the formation of functional organs. Genes controlling PCP have been extensively studied in *Drosophila*, revealing a crucial role for *frizzled* (*fz*) signaling through *dishevelled* (*dsh*) during the course of PCP establishment. The downstream components of the Fz/PCP pathway include RhoA, Drok, the JNK cascade and several other genes, most of which act tissue specifically (Adler, 2002; Mlodzik, 2002). Recent work has demonstrated that many of the genes involved in PCP signaling are also required for polarized morphogenetic cell movements such as convergent extension during early vertebrate embryogenesis (Fanto and McNeill, 2004; Mlodzik, 2002; Strutt, 2003; Wallingford et al., 2002). Habas et al. (Habas et al., 2001) suggested that the novel FH2 protein Daam1 is required for convergent extension is *Xenopus* embryos and that Daam1 might function as a bridging factor between Dsh and RhoA. Moreover, Wnt/Fz-mediated activation of RhoA appeared to depend on Dvl (a Dsh homolog) and Daam1 (Habas et al., 2001). However, in contrast to this model, previous work has provided evidence that formins act as Rho effectors downstream of the Rho GTPases (reviewed by Wasserman, 1998).

To gain further insights into the function of this novel class of FH2 proteins, we analyzed the single *Drosophila* member of the DAAM family (*DAAM*). Phenotypic analysis of *DAAM* mutants showed that it plays either no role or possibly a redundant role in PCP establishment in *Drosophila*. However, we found evidence that *DAAM* is involved in the regulation of the actin cytoskeleton in several different tissues, including the tracheal system. The *Drosophila* tracheal network is one of the best characterized model

[1]Institute of Genetics, Biological Research Center, Hungarian Academy of Sciences, H-6726 Szeged, Temesvári krt. 62, Hungary. [2]Brookdale Department of Molecular, Cell and Developmental Biology, Mount Sinai School of Medicine, One Gustave L. Levy Place, New York, NY 10029, USA. [3]European Molecular Biology Laboratory, Meyerhofstrasse 1, 69117, Heidelberg, Germany.

*Authors for correspondence (e-mail: mihaly@brc.hu; marek.mlodzik@mssm.edu)

Accepted 28 December 2005

systems of branching morphogenesis (Affolter and Shilo, 2000; Uv et al., 2003). During the first phase of tracheal development, the primordial cells invaginate in each embryonic hemisegment from the epidermis, migrate and undergo cell shape changes to form the primary branches (Affolter and Shilo, 2000; Manning, 1993; Uv et al., 2003). Subsequently, some tracheal branches fuse with an adjacent branch to build up a continuous tubular network. This process is mediated by fusion cells located at the branch tips, which recognize each other in the adjacent hemisegments and become doughnut shaped, forming a lumen that connects the two branches (Samakovlis et al., 1996). Before the end of embryogenesis, tracheal cells secrete a cuticle on their apical, luminal surface that protects the larvae from dehydration and infection. The tracheal cuticle is distinguished from the epidermal cuticle by the presence of cuticle ridges, often called taenidial folds that are thought to prevent the collapse of tracheal tubes while allowing them to expand and contract along their length.

Here, we show that *DAAM* is required to organize an array of parallel running actin cables beneath the apical surface of the tracheal cells that define the taenidial fold pattern of the cuticle. We found that the actin ring pattern corresponds exactly to that of the taenidial fold pattern, and we propose that the actin rings organized by *DAAM* define the position of taenidial fold formation. Our genetic interaction and epistasis data are consistent with a model that *DAAM* activity is regulated by *RhoA*. In addition, we show that DAAM works together with the non-receptor tyrosine kinases *Src42A* and *Tec29* to regulate the actin cytoskeleton of the *Drosophila* tracheal system.

MATERIALS AND METHODS

Fly strains and genetics

Excision alleles of *DAAM* were generated by remobilization of two P-element insertions, *EP(1)1336* and *EP(1)1542*. 300-300 dysgenic males were crossed individually to *y,w,l(1)/y,w,FM6* females to recover excisions, and establish stocks subsequently. Eye clones were induced by crossing *y,w,FRT19A, arm-lacZ/FM6; ey-Flp* males to $DAAM^{Ex68}$, *w, FRT19A/ y,w,FM6* females. In phenotypic rescue experiments, *Act-GAL4<UAS-FL-*$DAAM^{13.59}$*/CyO,Act-GFP*; *tub-GAL4<UAS-FL-*$DAAM^{13.59}$*/CyO,Act-GFP*; or *btl-GAL4<UAS-FL-*$DAAM^{13.59}$*/CyO,Act-GFP* males were crossed to females of different *DAAM* alleles. Rescue was examined in the male progeny, $DAAM^{Ex68}$ was rescued to adult viability in 25.8% of the appropriate males, while $DAAM^{Ex65}$ was rescued in 93.6% of the males.

For gain-of-function and epistasis analysis, UAS-C-DAAM/TM3,Sb,Kr-GFP; $Src42A^{E1}$/CyO,Act-GFP; UAS-C-DAAM/TM3,Ser,Act-GFP; $Tec29^{5610}$<FRT40A/ CyO,Act-GFP; UAS-C-DAAM/TM3, Ser,Act-GFP; $RhoA^{72F}$/ CyO,Act-GFP; UAS-C-DAAM/TM3,Ser,Act-GFP stocks were established and crossed to btl-GAL4 (on II) homozygous females. In co-expression experiments btl-GAL4<UAS-FL-$DAAM^{13.59}$/CyO,Act-GFP was crossed to UAS-C-DAAM/TM3,Sb,Kr-GFP. The appropriate genotypes were selected by the loss of GFP expression. For live imaging, embryos were collected from the progeny of a btl-GAL4 to UAS-actin::GFP/CyO cross.

In addition, we used the following mutant alleles: w^{1118}, Oregon-R, w,Df(1)AD11/FM7c (BL#1098), w,Df(1)AC7/FM7c (BL#1144), Tp(1;3)sta sta^{1}:ss^{sta}/FM3 (BL#844), and y^{1},l(1)EFd^{5}/Dp(1;Y)Sz280, y^{2}/FM6, l(1)11^{11} (BL#6021)

DNA techniques and transgenic constructs

Breakpoints of the excisions were mapped by standard Southern blot and PCR analysis. For overexpression and rescue experiments the UAS-FL-DAAM construct has been created by inserting the full-length RE67944 cDNA into the pUASp vector, while the UAS-C-DAAM construct carries a PCR amplified C-terminal region of the cDNA in the same pUASp vector encoding amino acids 518-1153. The polyclonal anti-DAAM antibody was raised in rabbit injected with a bacterially produced and purified His-tagged C-DAAM protein. After four boosts, the crude serum was used for immunostaining.

Immunohistochemistry and RNA in situ hybridization

For RNA in situ hybridization, probe was prepared by the DIG RNA Labelling Kit (Roche). Fixation and whole-mount embryo hybridization was carried out according to standard protocols. For immunofluorescence staining, the following antibodies were used: rat anti-DCAD2 1:10 (DSHB), rabbit anti-DAAM 1:4000, rat anti-Elav 1:300, mouse anti-β-gal 1:1000 (Promega), mouse anti-GFP 1:1000, mouse anti-2A12 1:5 (DSHB) and Rhodamine phalloidin at 1:100 (Molecular Probes). Secondary antibodies were: anti-rabbit-Alexa546, 1:500; anti-rabbit-Cy5, 1:300; anti-mouse-Alexa488, 1:500; anti-rat-Cy5, 1:300; anti-rat-Alexa488, 1:500; anti-mouse-Alexa488, 1:500 (all from Molecular Probes); and anti-mouse-biotinylated IgM 1:300 (Vector Laboratories). Embryos and larval tracheas were mounted in glycerol/PBS 4:1. Fluorescent and DIC images were collected using Zeiss LSM 510 and Olympus FV500 confocal microscopes. Bright-field images were collected using Zeiss Axiocam on Zeiss Axioskop MOT2. Images were assembled in Adobe Photoshop 7.0, GIMP 2.2.6 and ImageJ 1.32.

RESULTS

The *Drosophila* DAAM ortholog and the isolation of *DAAM* mutants

A recently published phylogenetic analysis (based on sequence comparisons of 101 FH2 domains from 26 eukaryotic species) has concluded that metazoan formins can be grouped into seven major subclasses (Higgs and Peterson, 2005). This analysis suggested that the DAAM subfamily clearly represents a distinct class. This is consistent with the previous finding that the DAAM subfamily exhibits extensive sequence similarity both within and outside of their highly conserved FH1 and FH2 domains (Habas et al., 2001). At present, however, very little is known about the in vivo function of the DAAM subfamily. Sequence analysis revealed the presence of a single DAAM ortholog in the *Drosophila* genome corresponding to the annotated gene CG14622 (Fig. 1A). Although the integrated *Drosophila* database (FlyBase) predicts that this gene might code for several different transcript classes, we focused our work on the predicted CG14622-RB transcript that appears to be encoded by the RE67944 EST clone (Fig. 1A). Sequencing of this full-length cDNA clone indicated a protein consisting of 1153 amino acids. Further analysis revealed that the ORF contains several conserved domains including an FH1, FH2, GBD and a putative DAD domain characteristic of formins. Based on the overall homology level and the phylogenetic analysis of FH2 domains (Higgs and Peterson, 2005), the DAAM subfamily appears to be most related to the Dia subfamily, raising the possibility that similar to the DRFs, DAAM formins are also regulated by an autoinhibitory mechanism that can be relieved upon RhoGTP binding.

To begin the functional analysis of *DAAM*, we generated loss-of-function mutant alleles by using two transposon insertions, *EP(1)1336* and *EP(1)1542*, in the immediate vicinity of the *DAAM* locus (Fig. 1A). Remobilization of these insertions allowed us to isolate a set of deletion alleles, two of which were mapped to the 5′ region of *DAAM*, and five of them were mapped to the 3′ region. The large 5′ deletions affect only 5′ UTR exons and intronic sequences (Fig. 1A), while the 3′ alleles carry smaller deletions (965-2538 bp), but affect the *DAAM* ORF, leading to C-terminal truncations that (depending on the allele) remove up to 457 amino acids of the predicted protein (Fig. 1B). All 5′ and 3′ deletion alleles are lethal as hemi- or homozygotes, with the exception of $DAAM^{Ex1}$, the smallest C-terminal deletion allele which is semiviable and fertile (viability is 17% when compared with wild type). The lethal 5′ and 3′ deletion alleles do not complement each other and the deficiencies uncovering this region [*Df(1)AD11*, *Df(1)AC7* and *Df(1)sta*]. They are, however, complemented by

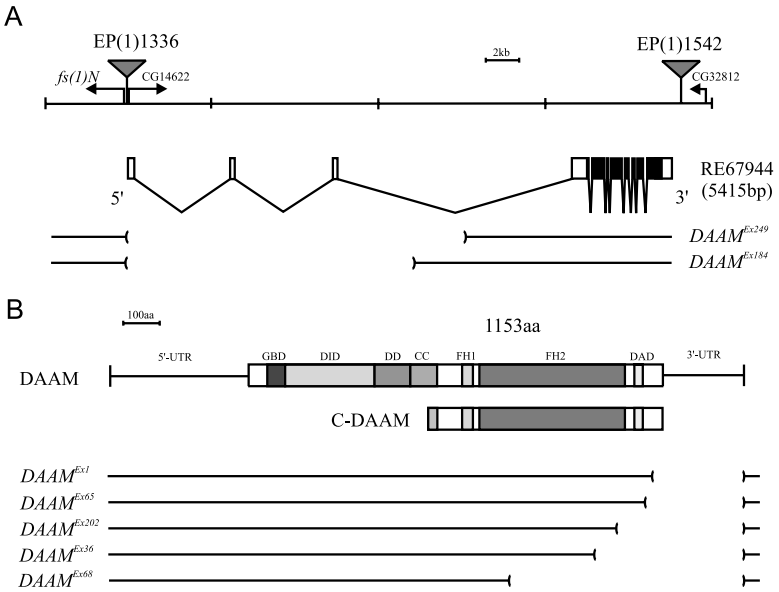

Fig. 1. The organization of the *DAAM* locus and the isolation of *DAAM* mutations. (**A**) The 1F2-3 cytological region includes the predicted gene CG14622 that we named *DAAM*. Position of two P-element insertion are shown, EP(1)1336 and EP(1)1542, which have been used to generate *DAAM* loss-of-function alleles including large 5′ deficiencies. The full-length cDNA clone RE67944 consists of 12 exons, translation starts in exon 4. (**B**) The full-length DAAM cDNA clone carries a 1165 bp 5′ UTR and a 731 bp 3′ UTR, and encodes a predicted protein of 1153 amino acids, which contains several homology domains, including GBD (GTPase binding domain), DID (Diaphanous inhibitory domain), DD (dimerization domain), CC (coiled-coil region), FH1 (formin homology domain 1), FH2 (formin homology domain 2) and DAD (Diaphanous autoinhibitory domain). The activated form of *DAAM* (C-DAAM) includes the C-terminal 637 amino acids of the protein. The position of the 3′ deficiency alleles is shown at the bottom.

Dp(1;3)sta and *Dp(1;Y)Sz280*, two transpositional duplications that carry the 1F2-3 cytological region, including *DAAM*. All lethal alleles are viable over $Daam^{Ex1}$, the weakest and homozygous viable allele, with the exception of the two largest C-terminal deficiency alleles ($Daam^{Ex68}$ and $Daam^{Ex36}$). To demonstrate that the lethality associated with these alleles is solely due to the lack of *DAAM*, transgenic flies carrying *UAS-FL-DAAM* (containing the full length RE67944 cDNA clone) were generated and tested in rescue experiments. When *UAS-FL-DAAM* was expressed under the control of *Act-Gal4* or *tub-Gal4* in a *DAAM* mutant background lethality was rescued to adult viability, even in case of the largest deletion allele $Daam^{Ex68}$. Taken together, these results demonstrate that all lethal alleles represent *DAAM* alleles and these mutations do not affect other essential genetic elements.

DAAM is unlikely to be required for PCP signaling in *Drosophila*

Based on biochemical assays and tissue culture experiments it was suggested that a human DAAM family member, DAAM1, is required for non-canonical Wnt/Fz signaling, and might function as a bridging factor between Dsh and RhoA. *Xenopus* embryo experiments supported this view, as the *Xenopus* ortholog xDaam1 has been implicated in PCP signaling during the early steps of gastrulation (Habas et al., 2001). To test whether the *Drosophila* DAAM is involved in PCP signaling, we carried out a loss-of-function analysis of the gene. We have thus induced *DAAM* mutant clones in the wing and compound eye, two PCP organization model tissues. Although several alleles were tested, none of them exhibited PCP defects in the eye or wing (not shown). The same was observed in adult escapers of the $DAAM^{Ex1}/DAAM^{Ex249}$ allelic combination.

We have also tested whether the PCP gain-of-function phenotypes induced by overexpression of PCP proteins can be modified by *DAAM* mutant alleles. To achieve this, we have compared the effects of Fz and Dsh overexpression in the wing or eye in wild-type and $DAAM^{Ex68}$ heterozygous mutant backgrounds. No significant difference between the wild-type and the *DAAM* mutant backgrounds was observed (not shown). Thus, the loss-of-function analysis of *DAAM* argues that the *Drosophila* DAAM ortholog is either not required for PCP signaling or at best plays a redundant role during PCP establishment.

DAAM regulates the formation of taenidial folds in the cuticle of the trachea

As the *DAAM* alleles are lethal, it encodes a gene with essential function(s). To identify these, we examined *DAAM* mutant larvae, and noticed that these animals display severe trachea defects. These include the collapse and flattening of the tracheal tubes, in both the main airways and the side branches (Fig. 2B,C). Wild-type tracheal cells secrete a cuticle on their apical (luminal) surface, which is continuous with the epidermal cuticle. Nevertheless, it is easily distinguished by the presence of cuticle ridges called taenidial folds that project into the lumen (Fig. 2A,B). These ridges form annular rings or run a helical course around the lumen of the tubes. Tracheal tubes of *DAAM* mutant larvae fail to secrete such a highly ordered cuticle. Instead, although some local order is visible, we observed short and curvy apical ridges that rarely run perpendicular to the tube axis (Fig. 2C,D). These striking cuticle pattern defects are detected throughout the tracheal system independent of tube types, with the exception of the fusion cells that secrete a different type of cuticle characterized by a dotty pattern instead of taenidial folds (see below, Fig. 5C). To confirm that the trachea phenotype is caused by *DAAM* loss of function, we expressed a *UAS-FL-DAAM* construct under the control of a trachea specific *btl-Gal4* driver. This significantly rescued the trachea disruptions (Fig. 2E), just as a general driver (e.g. *Act-Gal4*, not shown).

Next, we examined the expression of *DAAM* and confirmed that the mRNA is expressed in the developing embryonic tracheal system, starting from stage 13 of embryogenesis onwards (Fig. 3A). Similarly, immunostaining experiments (using a polyclonal anti-DAAM serum raised against the C-terminal half of the protein; see Materials and methods for details) revealed the presence of the DAAM protein in the developing embryonic tracheal cells in stage 13 and older embryos (Fig. 3B). In $DAAM^{Ex68}$ embryos, the antibody failed to detect protein in the trachea (Fig. 3D). Similarly, detectable protein was absent from mutant clonal tissue in eye-antennal imaginal discs, where *DAAM* is expressed during later stages of development (Fig. 3E-H). This confirmed that the antibody is specific to DAAM, and that $DAAM^{Ex68}$ is likely to be a protein null. Consistently, the trachea phenotype of $DAAM^{Ex68}$ homo- or hemizygous larvae is very similar to that of $DAAM^{Ex68}/Df(1)AD11$ larvae (Fig. 2E).

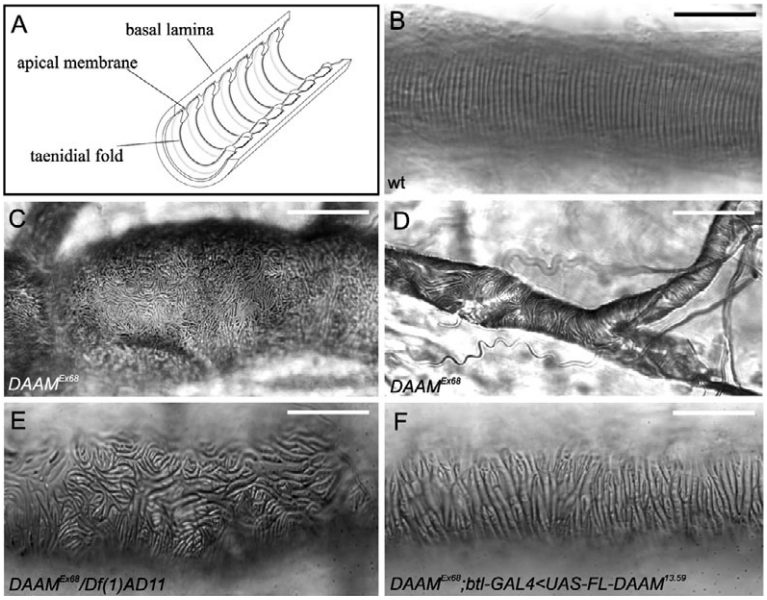

Fig. 2. The cuticle structure of wild-type and *DAAM* mutant *Drosophila* tracheal tubes. Schematic drawing of a wild-type main airway (**A**) shows that tracheal cuticle is laid down on the inner apical surface of tracheal cells. The cuticle is characterized by taenidial folds, running perpendicular to the tube axis, that are clearly visible on a native tracheal tube dissected out from a third instar larvae (**B**). The tracheal tubes of a *DAAM*^{Ex68} homozygous mutant larvae exhibit a strongly impaired cuticle pattern in both the main airways (**C**) and the side branches (**D**), often leading to the collapse of the tubes. (**E**) The trachea phenotype of *DAAM*^{Ex68} over *Df(1)AD11* (a deficiency that uncovers *DAAM*) is as strong as that of the homozygous *DAAM*^{Ex68} phenotype (compare E with C). (**F**) *btl-Gal4*-driven overexpression of the full-length *DAAM* protein (*FL-DAAM*$^{13.59}$) partly rescues the tracheal cuticle defects induced by *DAAM*^{Ex68}. Scale bars: 50 μm.

Actin organization in wild type and *DAAM* mutant tracheal tubes

As it is well established that formins regulate the actin cytoskeleton, we investigated actin organization in wild-type and *DAAM* mutant tracheal cells. This revealed that in wild-type tracheal cells apically localized actin is organized into parallel bundles running perpendicular to the axis of the tubes (Fig. 4A,C,E), strongly resembling the organization of teanidial folds in the cuticle. Significantly, the number of actin rings and taenidial folds in a given tracheal region is equal to each other (Fig. 4A-B). To determine precisely the time when such actin rings or spirals become apparent, we have expressed an Actin-GFP (green fluorescent protein) fusion protein in the trachea of living embryos (using the *btl-Gal4* tracheal driver line). This demonstrated that actin rings are first visible in late stage 15 embryos, just before the onset of cuticle secretion (Fig. 4N).

The embryonic tracheal cells are rather small, and thus it was difficult to study the formation of these actin rings at the subcellular level. Nevertheless, it is clear that these actin rings are not only present when cuticle secretion begins, but are also detected through the third larval instar stage. In contrast to the remarkable actin organization found in wild-type tracheal cells, in *DAAM*^{Ex68} mutants this organization is completely abolished. Whereas the absence of *DAAM* does not appear to reduce the apical F-actin level of the tracheal cells, actin cables formed are much shorter and thinner than in wild type (Fig. 4L,M). Additionally, actin bundles often appear to be crosslinked to each other instead of running parallel (Fig. 4L). Taken together, in *DAAM*^{Ex68} the actin bundles in the tracheal cells display abnormal morphology and fail to be organized into parallel running actin rings under the apical surface of the cells.

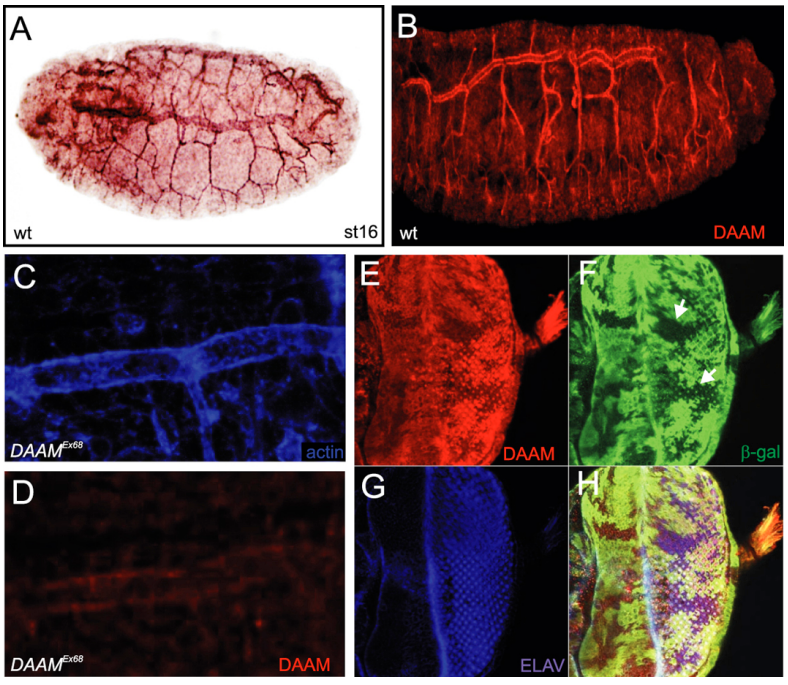

Fig. 3. *DAAM* expression in the embryonic tracheal system and the DAAM antibody. RNA in situ hybridization of *DAAM* (**A**) and immunohistochemical staining with a polyclonal anti-DAAM serum (**B**) revealed a strong expression in the developing embryonic tracheal system. Brown staining in A and red staining in B show *DAAM* expression in a stage 16 embryo. The anti-DAAM serum barely detects any DAAM protein in a *DAAM*^{Ex68} homozygous mutant embryonic trachea (**C**,**D**) and in mitotic clones induced in *DAAM*^{Ex68}, *w*, *FRT19A*/ *w*, *arm-lacZ*, *FRT19A*; *ey-flp*/+ larval eye imaginal disc [**E-H**; homozygous mutant clones (white arrows) lack DAAM staining]. Clones are marked by absence of β-gal (green). Elav (blue) is a neuronal marker. H is the merge of E-G. Anterior is towards the left, and dorsal is upwards in all panels.

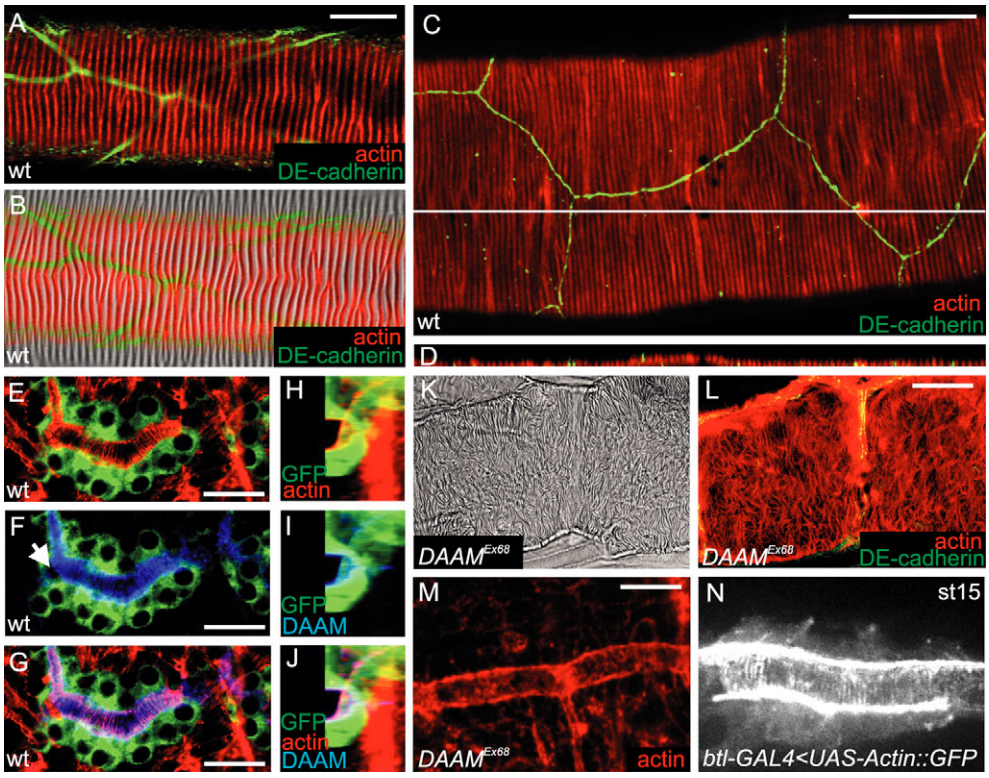

Fig. 4. *DAAM* is required to organize apical actin into parallel running bundles in tracheal cells. In a wild-type (wt) tracheal tube, actin is organized into parallel running bundles that are perpendicular to the tube axis (**A**). The number and phasing of these actin bundles correspond to the taenidial fold pattern displayed on the tracheal cuticle (**B**). Actin bundles formed in the tracheal cells are located at the level of the adherens junctions (**C**,**D**). (C) A confocal projection of a wild-type tracheal tube where actin is visualized in red, while the adherens junctional marker, DE-cadherin is shown in green. (D) An optical *xz* section along the white line in C, apical is at the top. (**E-G**) The DAAM protein is largely colocalized with actin in the embryonic tracheal cells. Confocal sections have been collected from a one-segment wide region of the dorsal trunk of a stage 16 embryo. The cytoplasm of tracheal cells is labeled with GFP in green, actin is shown in red, DAAM is in blue. Arrow in F indicates the fusion cells located at the segmental boundary. DAAM is not expressed in these cells. (**H-J**) 3D projections of the same confocal sections shown in E-G. Sections were rotated within the XZ plane by 90°. There is strong colocalization of actin and DAAM at apical membranes of the tracheal tubes (J). In $DAAM^{Ex68}$ mutant tracheal tubes, not only is the cuticle pattern impaired (**K**), but actin organization is also severely altered in both the larval (**L**) and embryonic (**M**) tracheal cells. Actin cables formed are thinner and shorter than their wild-type counterparts (compare A with L, and E with M), and fail to organize into regularly aligned bundles. The formation of the apical actin bundles in the embryonic tracheal cells (marked by actin::GFP) is first detected at approximately 13 hours AEL (**N**). Scale bars: 20 μm in A for A,B; 50 μm in C for C,D; 50 μm in L for K,L; 10 μm in E-G for E-J; 10 μm in M for M.

Although the global actin organization is severely impaired, local order can often be detected in small patches within a cell. The cuticle pattern of $DAAM^{Ex68}$ mutants displays a similar phenotype, indicating that actin cables direct the run of taenidial folds, even in the *DAAM* mutant situation. Thus, it appears that the major function of *DAAM* in *Drosophila* tracheal cells is to organize an array of actin rings that directs cuticle patterning by specifying the site of taenidial fold formation. Despite the fact that the apical actin level is not significantly reduced in *DAAM* mutants, we cannot exclude the possibility that in the wild-type situation, *DAAM* also contributes to actin assembly, a well characterized formin function. Consistent with this possibility, DAAM largely colocalizes with the apically enriched actin bundles in the embryonic trachea cells (Fig. 4E-J). Nevertheless, the potential involvement in actin polymerization appears be a redundant function. The recently characterized *form3* is the best candidate to be functionally redundant with *DAAM* for actin assembly, because it is the only other *Drosophila* formin known to be expressed in the tracheal system (Tanaka et al., 2004).

Activated DAAM interferes with cuticle patterning in tracheal cells and transforms the cuticle pattern of the fusion cells

Truncated formins consisting only of the C-terminal FH1 and FH2 domains behave as constitutively active forms in many contexts (Evangelista et al., 1997; Habas et al., 2001; Tominaga et al., 2000; Watanabe et al., 1999). To test whether DAAM activity is regulated in a similar manner, *UAS-C-DAAM* (carrying a truncated *DAAM* encoding the C-terminal 637 amino acids including the FH1 and FH2 domains; Fig. 1B) transgenic flies were generated. Strikingly, C-DAAM expressed in the trachea (with the *btl-Gal4* driver) caused distinct phenotypic effects in the fusion cells and the regular tracheal cells.

After the cuticle is laid down in the tracheal system, fusion cells are easily distinguished from others because these narrow, doughnut-shaped cells have a characteristic granulated cuticle pattern that is very distinct from the parallel running apical ridges (Fig. 5C). The same difference can be found at the level of actin organization, as apical actin is also concentrated into a granular pattern (Fig. 5D). Significantly, anti-DAAM staining in wild type revealed that fusion cells, unlike the normal tracheal cells, do not express DAAM (Fig. 4F,G). When C-DAAM is expressed in fusion cells it induces a dramatic change in the actin organization and cuticle pattern, causing strong actin accumulation at the apical surface. However, most of the actin is found in largely unorganized bundles (Fig. 5F), although the typical granular pattern is barely visible. In addition, such fusion cells are often wider than their wild-type counterparts, and their granular cuticle pattern is transformed towards a stripy pattern, partly resembling the taenidial folds of normal tracheal cells (Fig. 5E). However, when full-length DAAM was expressed in the fusion cells (or elsewhere in the tracheal system) we could not detect any phenotypic effects (not shown).

Several conclusions can be drawn from these data. First, C-DAAM behaves as an activated formin, consistent with its domain structure and showing that the activity of DAAM is regulated by N-

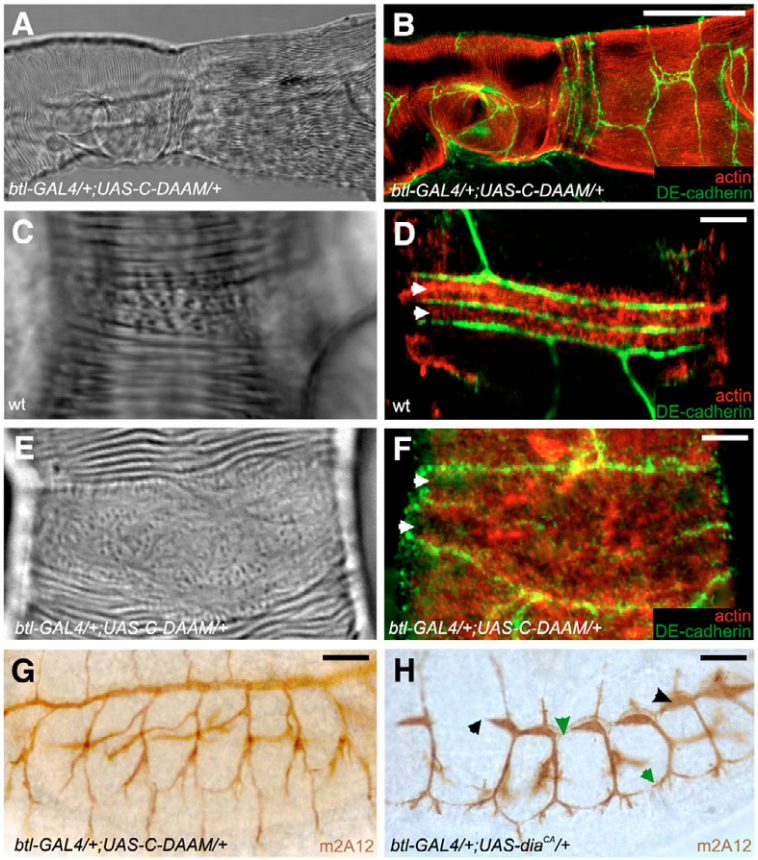

Fig. 5. The trachea specific overexpression of activated forms of DAAM and Dia. Btl-Gal4 driven expression of C-DAAM (activated DAAM) affects the cuticle pattern (**A**) and impairs actin organization in the tracheal system (**B**). Fusion cells are narrow doughnut-shaped cells that are easily distinguished from the regular tracheal cells by their spotted cuticle pattern (**C**). Actin in fusion cells (red) is also concentrated into a spotted pattern (**D**). When C-DAAM is ectopically expressed in the fusion cells, it often induces a change in their shape, and leads to a partial transformation of the spotted cuticle towards the taenidial fold pattern (**E**). Additionally, we detected a strong actin accumulation in the fusion cells where short actin bundles are often visible (**F**). DE-cadherin labels the cell boundaries on B,D,F; arrows indicate the fusion cells on D and F. C and D are the same wild type larval trachea, E and F are from the same DAAM overexpressing trachea. Whereas, C-DAAM expression in the tracheal network does not significantly alter the general structure of the tubular system (**G**), the presence of Dia^{CA} (an activated form of *diaphanous*) leads to fusion defects in the dorsal trunk (black arrow), constrictions at the fusion cells (green arrowhead), widening at other areas of the dorsal trunk (black arrowhead) and impairments of terminal branch differentiation (green arrow) (**H**). The tracheal system in G and H is visualized by the luminal antibody 2A12. Scale bars: 50 μm in B for A,B;10 μm in D for C,D; 10 μm in F for E,F; 10 μm in G,H.

terminal sequences like the DRF subfamily. Second, although actin cables polymerized by C-DAAM failed to organize into such perfect rings as found in wild-type tracheal cells, C-DAAM plays an instructive role in cuticle secretion by polymerizing actin cables that are sufficient to change the cuticle pattern in a *DAAM* non-expressing cell towards the pattern characteristic of *DAAM*-expressing cells. Third, the mere presence of DAAM is not sufficient to change the cuticle pattern of fusion cells, only the activated form can do that, suggesting that fusion cells lack the activator(s) of this formin.

Overexpression of C-DAAM in normal tracheal cells (where the endogenous wild-type DAAM is expressed) resulted in severe impairment of taenidial fold formation and actin organization (Fig. 5A,B) in a qualitatively similar manner to the absence of *DAAM*. Recent results indicated that formins normally act in dimeric or multimeric forms (Li and Higgs, 2003; Otomo et al., 2005a; Otomo et al., 2005b; Rose et al., 2005; Takeya and Sumimoto, 2003; Xu et al., 2004; Zigmond et al., 2003). It has also been demonstrated that homotypic protein interaction of the mammalian formin, Fhos, is mediated by the FH2 domain, and an FH1-FH2 (C-DAAM equivalent) Fhos fragment is able to bind the full-length protein (Takeya and Sumimoto, 2003). Therefore, it was possible that the *btl-Gal4/UAS-C-DAAM* phenotype is, at least partly, caused by an antimorphic effect of C-DAAM by interfering with the wild-type protein through dimerization. In that case, it is expected that increasing wild-type DAAM levels will suppress the *btl-Gal4/UAS-C-DAAM* phenotype.

To test this hypothesis, we examined *btl-Gal4* driven co-expression of FL-DAAM and C-DAAM. This caused a strong suppression of the *btl-Gal4/UAS-C-DAAM* phenotype in regular tracheal cells (Fig. 7E), but not in fusion cells (not shown). These data indicate that C-DAAM indeed behaves as an antimorph in regular tracheal cells. In fusion cells, however, the lack of suppression by expressing FL-DAAM is consistent with *DAAM* having no endogenous function in these cells. Because the UAS-Gal4 system usually induces a robust expression, C-DAAM is likely to be in excess when compared with endogenous DAAM in *btl-Gal4/UAS-C-DAAM* tracheal cells. Thus, the tracheal phenotype in the regular tracheal cells is possibly the sum of two effects: an antimorphic effect through interference with the endogenous protein and a neomorphic effect through an excess of activated C-DAAM, which increases actin polymerization rate but fails to organize actin bundles properly. An alternative hypothesis to explain that C-DAAM overexpression leads to similar phenotypic effects to the loss of *DAAM,* could be that the amount of F-actin produced by C-DAAM exceeds the actin organizing capacity of endogenous DAAM. As we could not detect higher levels of apical actin in these tracheal cells, we favor the first hypothesis.

The precise mechanism by which C-DAAM impairs actin organization and cuticle patterning in tracheal cells is unclear. It is remarkable that although activated DAAM is lacking most of the formin regulatory domains, it was specific and only disrupted cuticle patterning without affecting other biological processes in the trachea (Fig. 5G). By comparison, expression of a constitutively activated form of *dia* (Dia^{CA}), the most closely related *Drosophila* formin to *DAAM*, destroys the normal branching pattern of the tracheal tubes (Fig. 5H). In addition, dorsal trunk fusion is often blocked and tracheal cuticle is not secreted (Fig. 5H). Thus, it appears that Dia^{CA} has an earlier effect on trachea development than C-DAAM. Together, these results suggest that DAAM carries a highly specific trachea function that is restricted to the assembly and organization

of apical actin cables, which direct cuticle patterning, with most of the functional specificity coming from the C-terminal FH1-FH2 domains.

DAAM interacts with *RhoA* and Src family non-receptor tyrosine kinases

To gain insights into the regulation of DAAM and to identify potential partners that work together with DAAM to organize apical actin in tracheal cells, we carried out a genetic interaction test with a panel of cytoskeleton regulators known to be expressed in the *Drosophila* respiratory system. We used the weak hypomorphic $DAAM^{Ex1}$ allele that exhibits a mild phenotype (Fig. 6A), and thus appears to be the most appropriate for dominant genetic interaction assays. This approach identified *RhoA*, and two Src family non-receptor tyrosine kinases, *Src42A* and *Tec29*, as strong enhancers of the $DAAM^{Ex1}$ phenotype (Fig. 6B-D). To test whether these interactors have tracheal cuticle patterning phenotypes on their own, we examined the trachea of their homozygous mutant embryos and larvae. In agreement with the observation that *btl-Gal4* driven expression of dominant-negative *RhoA* ($RhoA^{N19}$) blocks lumen formation (Lee and Kolodziej, 2002), we found that absence of *RhoA* arrests tracheal development before dorsal trunk fusion takes place (not shown). Therefore, it was not possible to assess directly the effect of *RhoA* single mutants on apical actin organization and/or cuticle structure. However, although some of the very few hatching *Src42A* and *Tec29* mutant larvae displayed a tracheal necrosis phenotype, others displayed a superficially normal-looking tracheal tree, where cuticle secretion has been completed. These larvae die as first instar, and, strikingly, exhibit an abnormal taenidial fold pattern similar to that of *DAAM* mutant larvae (Fig. 6E-H). Although the $Tec29^{5610}$ and $Src42A^{E1}$ tracheal phenotypes are weaker than that of the *DAAM* null allele, consistent with our previous conclusion that apical actin organization determines the taenidial pattern, these mutations also affect apical actin bundles in the tracheal system (Fig. 6I,J). Thus, these results indicate that *Src42A* and *Tec29* are involved in taenidial fold patterning and during this process probably act together with *DAAM*. Significantly, the FH1 domain is known to bind SH3 proteins (Kamei et al., 1998; Tominaga et al., 2000; Vallen et al., 2000), and the Src family kinases have been implicated in several forming-related processes (Gasman et al., 2003; Tominaga et al., 2000). Additionally, we found that the *RhoA*, *Src42A* and *Tec29* mutations not only enhance the tracheal cuticle defects caused by *DAAM*, but also decreased the viability of the semilethal $DAAM^{Ex1}$ allele (not shown), suggesting that these proteins may work together in other tissues as well. The observation that *RhoA* is an enhancer of $DAAM^{Ex1}$ further supports the model that DAAM family formins are regulated by Rho GTPases, similar to the regulation of the DRF subfamily. These data are also consistent with the previous report demonstrating that RhoA is a direct binding partner of human DAAM1 (Habas et al., 2001). Surprisingly, however, $DAAM^{Ex1}$ does not show a genetic interaction with *dsh*, the *Drosophila* homologue of Dvl, another protein found to bind human DAAM1 (Habas et al., 2001). Although this result does not exclude the possibility that DAAM activation in the tracheal cells normally requires Dsh binding, a detailed analysis of the trachea function of *wg* signaling, including *dsh*, failed to reveal a tracheal cuticle defect (Llimargas, 2000), suggesting that Dsh is not involved in DAAM regulation in the trachea.

To further investigate the regulatory relationship between *DAAM* and its genetic interactors, we examined if the *btl-Gal4/UAS-C-DAAM* phenotype was sensitive to the gene dose of *RhoA*, *Src42A*

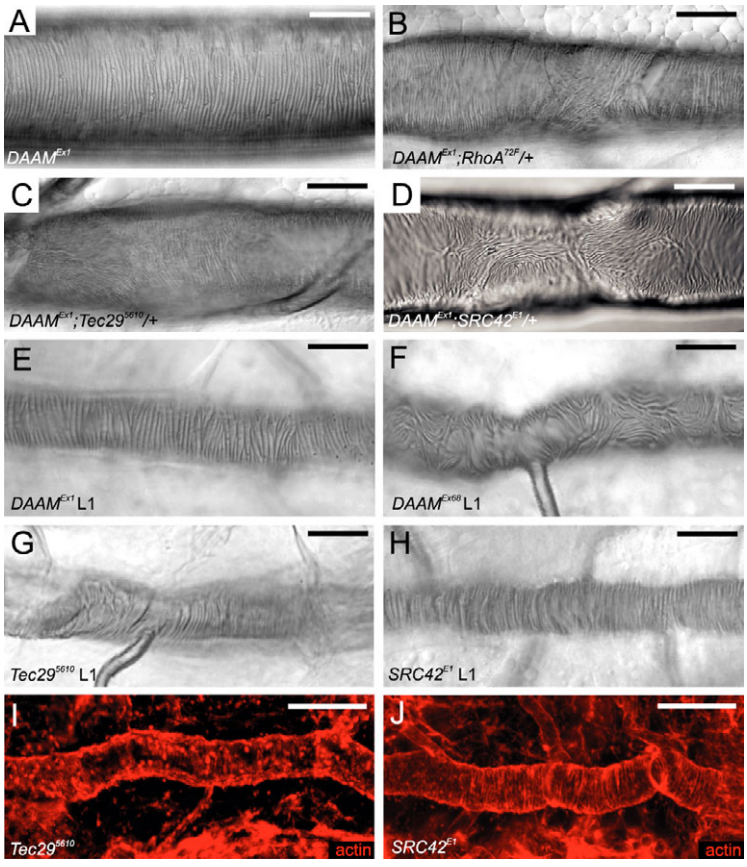

Fig. 6. The genetic interaction partners of *DAAM*. Trachea dissected out from third instar $DAAM^{Ex1}$ mutant larvae display a moderate cuticle phenotype (**A**), which is strongly enhanced by removal of one copy of *RhoA* (**B**), *Tec29* (**C**) and *Src42A* (**D**). The *DAAM* trachea phenotypes are already exhibited in first instar larvae (**E**,**F**). Homozygous mutant *Tec29* (**G**) and *Src42A* (**H**) first instar larvae display a moderately strong taenidial phenotype similar to $DAAM^{Ex1}$ (compare G and H with E). Consistent with this, apical actin organization is partly impaired in *Tec29* (**I**) and *Src42A* (**J**) mutant embryonic tracheal tubes (compare I and J with Fig. 4E). Scale bars: 50 μm in A-H; 10 μm in I,J.

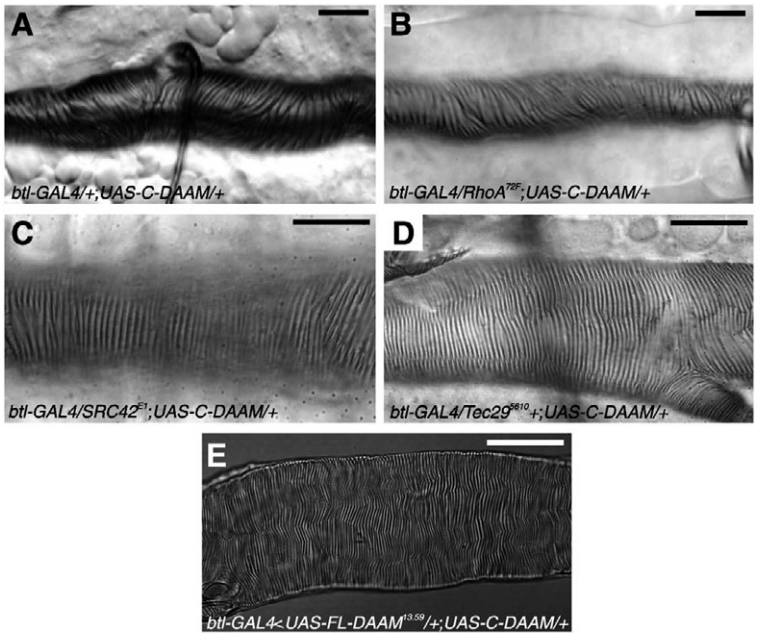

Fig. 7. Epistasis experiments with C-DAAM. Cuticle defects induced by C-DAAM expression in tracheal cells (**A**) are not modified by *RhoA* (**B**), but are strongly suppressed by *Src42A* (**C**), *Tec29* (**D**) and co-expression with the full-length form of *DAAM* (*FL-DAAM*$^{13.59}$) (**E**). Scale bars: 50 μm.

and *Tec29*. This epistasis analysis indicated that while *RhoA* did not modify the effect of C-DAAM expression, *Src42A* and *Tec29* dominantly suppressed the respective cuticle defects (Fig. 7A-D). These data are consistent with the model that *RhoA* is an upstream regulator of *DAAM*, whereas the non-receptor tyrosine kinases act downstream of or in parallel to it. Hence, these results further support the view that the DAAM family formins are regulated by Rho GTPases. With respect to non-receptor tyrosine kinases, our data support similar conclusions to those of previous reports, demonstrating that mouse Dia1 and mouse Dia2 act upstream of Src in the regulation of actin dynamics (Tominaga et al., 2000), and that human DIA2C is required for Src activation during the process of endosome regulation (Gasman et al., 2003).

DISCUSSION

Actin organization and cuticle structure in the *Drosophila* tracheal system

The basic structure of the insect tracheal system is a highly conserved tubular network in every species. The most important function of this network is to allow oxygen flow to target cells. Thus, tracheal tubes need to be both rigid enough, to ensure continuous air transport, and flexible enough along the axis of the tubes, to prevent the break down of the tube system when body parts or segments move relative to each other. These requirements are mainly ensured by the tracheal cuticle, which covers the luminal surface of the tubes and displays cuticle ridges (making the overall structure similar to the corrugated hose of a vacuum cleaner). Analysis of *DAAM* mutants provides the first direct evidence that this hypothesis is correct. Our data demonstrate that in the absence of *DAAM* the taenidial fold pattern is severely disrupted, often leading to the collapse of the tubes and to discontinuities in the tubular network. In addition, our analysis revealed that the remarkably ordered cuticle pattern, displayed in the wild-type trachea tubes, depends on DAAM-mediated apical actin organization. Apical actin is organized into parallel-running actin cables, much the same way teanidial folds run in the cuticle. Significantly, the formation of these actin bundles precedes the onset of cuticle secretion, and the number and phasing of the actin rings correspond exactly to that of the taenidial folds in the cuticle. Thus our studies revealed a novel aspect of apical actin organization in the tracheal cells that has not been appreciated before.

The *DAAM* gene encodes a novel member of the formin family of proteins, involved in actin nucleation and polymerization. Consistent with this, DAAM is colocalized with apical actin in the tracheal cells, and the activated form of DAAM is able to induce actin assembly when expressed in tracheal cells (this work) and in other cell types (T.M. and J.M., unpublished). In *DAAM* mutant tracheal cells, apical actin is still detected, albeit at a somewhat lower level than in wild type, but the bundles formed in the mutant are much shorter and thinner than in wild type, and often appear to be crosslinked to each other. Most strikingly, global actin organization is almost completely lost, although some local order can still be detected. Remarkably, the cuticle pattern in mutant tracheal cells still follows the underlying aberrant actin pattern. Overall, in *DAAM* mutants, both the tracheal cuticle and the apical actin pattern resemble a mosaic of locally ordered patches that failed to be coordinated and aligned with each other and the axis of the tracheal tubes. We thus propose that the apical actin bundles play a key role in patterning the tracheal cuticle by defining the place of taenidial fold formation. Regarding the function of DAAM, our results suggest that the major role of this formin in the tracheal cells is to organize the actin filaments into parallel running actin rings or spirals instead of simply executing the well characterized formin function related to actin assembly. However, whether this is a direct effect on actin organization, and thus represents a novel formin function, needs to be further elucidated. An alternative model could be that DAAM is primarily required for actin polymerization but tightly coupled to an actin ‘organizing’ protein. In such scenario, the polymerization activity should be a redundant requirement, whereas the link to the organizing protein would be a DAAM-specific function, thereby explaining the presence of unorganized actin bundles in *DAAM* mutant tracheal cells.

In the case of the main tracheal airways, which are multicellular along their periphery, it is striking that in wild type the run of the actin bundles is perfectly coordinated across cell boundaries. In addition, the run is always perpendicular to that of the tube axis.

How does *DAAM* ensure the coordination of these two aspects of actin organization? Because the DAAM protein and the apical actin cables are both found at the level of the adherens junctions, it is possible that DAAM regulates the coordination of the actin cables at the cell boundaries through a direct interaction with junctional protein complexes. However, other explanations are also possible, and further experiments will be required to elucidate the molecular mechanism of this regulatory function. The fact that actin cables normally run perpendicular to the tube axis seems to suggest that tracheal cells are able to sense a global orientation cue and align their actin bundles accordingly. The nature and source of this cue is unknown, as is the mechanism by which DAAM is involved in the read-out of this signal. Nevertheless, it is interesting that in *DAAM* and *btl-Gal4/UAS-C-DAAM* mutant trachea, the main pattern of the cuticle phenotype is often changing from one segment to the other, suggesting that the effect of the 'global' orientation cue is limited to metameric units.

Regulatory interaction between RhoA and DAAM

Sequence comparisons of FH2 proteins suggest a close phylogenetic relationship between the DRF, FRL and DAAM subfamilies (Higgs and Peterson, 2005). Members of these three subfamilies have a high level of conservation in the FH2 domain, and importantly, also in the region of the GBD and DAD domains, suggesting that the FRL and DAAM family formins are also regulated by autoinhibition and RhoGTPases, like the DRFs. We present further evidence in support of this view. First, *DAAM* and *RhoA* display a strong genetic interaction. Second, C-DAAM (an N-terminally truncated form of DAAM) behaves like an activated form much the same way DRF family formins behave. Third, epistasis experiments with C-DAAM and *RhoA* suggest that RhoA acts upstream of DAAM. Thus, our data support the model in which DAAM, at least in the *Drosophila* tracheal system, is regulated by autoinhibition that can be relieved by RhoGTPases.

This conclusion, however, contradicts the observation that human DAAM1 is required for Wnt/Fz/Dvl dependent RhoA activation in cultured cells and that xDaam1 appears to mediate Wnt-11 dependent RhoA activation in *Xenopus* embryos (Habas et al., 2001). These results suggested that DAAM functions upstream of RhoA in non-canonical Wnt/Fz-PCP signaling. An explanation for these distinct conclusions might be related to the fact that DAAM, in contrast to xDaam1, does not appear to be required for Fz/Dsh-PCP signaling. Hence, it is possible that the *Drosophila* ortholog is regulated in the same way as the DRF formins, while the vertebrate family members can be regulated in a different way, once bound by Dsh/Dvl and recruited into PCP signaling complexes.

DAAM cooperates with Src42A and Tec29 to regulate the tracheal cuticle pattern

Genetic interactions with the hypomorphic $DAAM^{Ex1}$ allele identified two non-receptor tyrosine kinases, *Src42A* and *Tec29*, as strong interacting partners. Although both of these kinases play multiple roles during embryogenesis, we demonstrate that single mutants for both affect the tracheal cuticle pattern in a similar way to *DAAM*. These results suggest that *DAAM* and the Src family kinases work together to regulate the actin cytoskeleton and cuticle pattern in tracheal cells. Although it is not known whether DAAM physically binds Src42A and/or Tec29, it has been established that the FH1 region of DRFs and other formins can bind SH3 domains, including those of the Src family kinases (Gasman et al., 2003; Tominaga et al., 2000; Uetz et al., 1996). In agreement with our data that *DAAM* acts upstream of Src42A and Tec29 in tracheal cells, cytoskeleton remodeling and SRF activation mediated by mouse Dia1 and mouse Dia2 requires Src activity (Tominaga et al., 2000). Moreover, a recent report suggests that RhoD and human DIA2C regulate endosome dynamics through Src activation, proposing that Src activity is stimulated via human DIA2C dependent recruitment to early endosomes (Gasman et al., 2003). Similarly, the Limb deformity protein (a formin) interacts with Src on the perinuclear membranes of primary mouse fibroblasts (Uetz et al., 1996). Based on these examples, we speculate that in *Drosophila* tracheal cells the RhoA/DAAM/Src module may not only be required to organize apical actin bundles, but additionally it might represent a link to secretory vesicles and to the regulation of exocytosis. Future studies will be required to test this hypothesis, and to unravel the mechanisms whereby DAAM family formins and Src family kinases contribute to cytoskeletal remodeling in the *Drosophila* tracheal system and in other tissues.

We thank M. Krasnow, P. Rorth, M. Affolter, the Developmental Studies Hybridoma Bank, the Bloomington Stock Center and the Szeged Stock Center for fly stocks and reagents. We are grateful to H. Gyurkovics, T. Török and J. Reynolds-Kenneally for critical reading and helpful comments on the manuscript. We are particularly grateful to Anna Rehák, Edit Gyányi and Edina Ördög for technical assistance. We thank L. Homolya and B. Sarkadi at the National Medical Center (Budapest) for their patience and generous help with microscopy facilities. This research was supported by NIH FIRCA grant TW05893 to M.M. and J.M., and by a NIH NIGMS RO1 grant GM62917 to M.M. J.M. is an EMBO/HHMI Scientist and a Bolyai János Research Scholar.

References

Adler, P. N. (2002). Planar signaling and morphogenesis in Drosophila. *Dev. Cell* **2**, 525-535.

Affolter, M. and Shilo, B. Z. (2000). Genetic control of branching morphogenesis during Drosophila tracheal development. *Curr. Opin. Cell Biol.* **12**, 731-735.

Alberts, A. S. (2001). Identification of a carboxyl-terminal diaphanous-related formin homology protein autoregulatory domain. *J. Biol. Chem.* **276**, 2824-2830.

Chan, D. C., Bedford, M. T. and Leder, P. (1996). Formin binding proteins bear WWP/WW domains that bind proline-rich peptides and functionally resemble SH3 domains. *EMBO J.* **15**, 1045-1054.

Chang, F., Drubin, D. and Nurse, P. (1997). cdc12p, a protein required for cytokinesis in fission yeast, is a component of the cell division ring and interacts with profilin. *J. Cell Biol.* **137**, 169-182.

Evangelista, M., Blundell, K., Longtine, M. S., Chow, C. J., Adames, N., Pringle, J. R., Peter, M. and Boone, C. (1997). Bni1p, a yeast formin linking cdc42p and the actin cytoskeleton during polarized morphogenesis. *Science* **276**, 118-122.

Evangelista, M., Pruyne, D., Amberg, D. C., Boone, C. and Bretscher, A. (2002). Formins direct Arp2/3-independent actin filament assembly to polarize cell growth in yeast. *Nat. Cell Biol.* **4**, 260-269.

Evangelista, M., Zigmond, S. and Boone, C. (2003). Formins: signaling effectors for assembly and polarization of actin filaments. *J. Cell Sci.* **116**, 2603-2611.

Fanto, M. and McNeill, H. (2004). Planar polarity from flies to vertebrates. *J. Cell Sci.* **117**, 527-533.

Gasman, S., Kalaidzidis, Y. and Zerial, M. (2003). RhoD regulates endosome dynamics through Diaphanous-related Formin and Src tyrosine kinase. *Nat. Cell Biol.* **5**, 195-204.

Habas, R., Kato, Y. and He, X. (2001). Wnt/Frizzled activation of Rho regulates vertebrate gastrulation and requires a novel Formin homology protein Daam1. *Cell* **107**, 843-854.

Higgs, H. N. and Peterson, K. J. (2005). Phylogenetic analysis of the formin homology 2 domain. *Mol. Biol. Cell* **16**, 1-13.

Imamura, H., Tanaka, K., Hihara, T., Umikawa, M., Kamei, T., Takahashi, K., Sasaki, T. and Takai, Y. (1997). Bni1p and Bnr1p: downstream targets of the Rho family small G-proteins which interact with profilin and regulate actin cytoskeleton in Saccharomyces cerevisiae. *EMBO J.* **16**, 2745-2755.

Kamei, T., Tanaka, K., Hihara, T., Umikawa, M., Imamura, H., Kikyo, M., Ozaki, K. and Takai, Y. (1998). Interaction of Bnr1p with a novel Src homology 3 domain-containing Hof1p. Implication in cytokinesis in Saccharomyces cerevisiae. *J. Biol. Chem.* **273**, 28341-28345.

Kohno, H., Tanaka, K., Mino, A., Umikawa, M., Imamura, H., Fujiwara, T., Fujita, Y., Hotta, K., Qadota, H., Watanabe, T. et al. (1996). Bni1p implicated in cytoskeletal control is a putative target of Rho1p small GTP binding protein in Saccharomyces cerevisiae. *EMBO J.* **15**, 6060-6068.

Lee, S. and Kolodziej, P. A. (2002). The plakin Short Stop and the RhoA GTPase are required for E-cadherin-dependent apical surface remodeling during tracheal tube fusion. *Development* **129**, 1509-1520.
Li, F. and Higgs, H. N. (2003). The mouse Formin mDia1 is a potent actin nucleation factor regulated by autoinhibition. *Curr. Biol.* **13**, 1335-1340.
Llimargas, M. (2000). Wingless and its signalling pathway have common and separable functions during tracheal development. *Development* **127**, 4407-4417.
Manning, G. and Krasnow, M. A. (1993). Development of the Drosophila tracheal system. In *The Development of Drosophila melanogaster*, *vol. I* (ed. M. Bate and A. Martinez-Arias), pp. 609-686. Plainview (NY): Cold Spring Harbor Laboratory Press.
Mlodzik, M. (2002). Planar cell polarization: do the same mechanisms regulate Drosophila tissue polarity and vertebrate gastrulation? *Trends Genet.* **18**, 564-571.
Otomo, T., Otomo, C., Tomchick, D. R., Machius, M. and Rosen, M. K. (2005a). Structural basis of Rho GTPase-mediated activation of the formin mDia1. *Mol. Cell* **18**, 273-281.
Otomo, T., Tomchick, D. R., Otomo, C., Panchal, S. C., Machius, M. and Rosen, M. K. (2005b). Structural basis of actin filament nucleation and processive capping by a formin homology 2 domain. *Nature* **433**, 488-494.
Pring, M., Evangelista, M., Boone, C., Yang, C. and Zigmond, S. H. (2003). Mechanism of formin-induced nucleation of actin filaments. *Biochemistry* **42**, 486-496.
Pruyne, D., Evangelista, M., Yang, C., Bi, E., Zigmond, S., Bretscher, A. and Boone, C. (2002). Role of formins in actin assembly: nucleation and barbed-end association. *Science* **297**, 612-615.
Rose, R., Weyand, M., Lammers, M., Ishizaki, T., Ahmadian, M. R. and Wittinghofer, A. (2005). Structural and mechanistic insights into the interaction between Rho and mammalian Dia. *Nature* **435**, 513-518.
Sagot, I., Klee, S. K. and Pellman, D. (2002a). Yeast formins regulate cell polarity by controlling the assembly of actin cables. *Nat. Cell Biol.* **4**, 42-50.
Sagot, I., Rodal, A. A., Moseley, J., Goode, B. L. and Pellman, D. (2002b). An actin nucleation mechanism mediated by Bni1 and profilin. *Nat. Cell Biol.* **4**, 626-631.
Samakovlis, C., Manning, G., Steneberg, P., Hacohen, N., Cantera, R. and Krasnow, M. A. (1996). Genetic control of epithelial tube fusion during Drosophila tracheal development. *Development* **122**, 3531-3536.
Shimada, A., Nyitrai, M., Vetter, I. R., Kuhlmann, D., Bugyi, B., Narumiya, S., Geeves, M. A. and Wittinghofer, A. (2004). The core FH2 domain of diaphanous-related formins is an elongated actin binding protein that inhibits polymerization. *Mol. Cell* **13**, 511-522.
Strutt, D. (2003). Frizzled signalling and cell polarisation in Drosophila and vertebrates. *Development* **130**, 4501-4513.
Takeya, R. and Sumimoto, H. (2003). Fhos, a mammalian formin, directly binds to F-actin via a region N-terminal to the FH1 domain and forms a homotypic complex via the FH2 domain to promote actin fiber formation. *J. Cell Sci.* **116**, 4567-4575.
Tanaka, H., Takasu, E., Aigaki, T., Kato, K., Hayashi, S. and Nose, A. (2004). Formin3 is required for assembly of the F-actin structure that mediates tracheal fusion in Drosophila. *Dev. Biol.* **274**, 413-425.
Tominaga, T., Sahai, E., Chardin, P., McCormick, F., Courtneidge, S. A. and Alberts, A. S. (2000). Diaphanous-related formins bridge Rho GTPase and Src tyrosine kinase signaling. *Mol. Cell* **5**, 13-25.
Uetz, P., Fumagalli, S., James, D. and Zeller, R. (1996). Molecular interaction between limb deformity proteins (formins) and Src family kinases. *J. Biol. Chem.* **271**, 33525-33530.
Uv, A., Cantera, R. and Samakovlis, C. (2003). Drosophila tracheal morphogenesis: intricate cellular solutions to basic plumbing problems. *Trends Cell Biol.* **13**, 301-309.
Vallen, E. A., Caviston, J. and Bi, E. (2000). Roles of Hof1p, Bni1p, Bnr1p, and myo1p in cytokinesis in Saccharomyces cerevisiae. *Mol. Biol. Cell* **11**, 593-611.
Wallar, B. J. and Alberts, A. S. (2003). The formins: active scaffolds that remodel the cytoskeleton. *Trends Cell Biol.* **13**, 435-446.
Wallingford, J. B., Fraser, S. E. and Harland, R. M. (2002). Convergent extension: the molecular control of polarized cell movement during embryonic development. *Dev. Cell* **2**, 695-706.
Wasserman, S. (1998). FH proteins as cytoskeletal organizers. *Trends Cell Biol.* **8**, 111-115.
Watanabe, N., Madaule, P., Reid, T., Ishizaki, T., Watanabe, G., Kakizuka, A., Saito, Y., Nakao, K., Jockusch, B. M. and Narumiya, S. (1997). p140mDia, a mammalian homolog of Drosophila diaphanous, is a target protein for Rho small GTPase and is a ligand for profilin. *EMBO J.* **16**, 3044-3056.
Watanabe, N., Kato, T., Fujita, A., Ishizaki, T. and Narumiya, S. (1999). Cooperation between mDia1 and ROCK in Rho-induced actin reorganization. *Nat. Cell Biol.* **1**, 136-143.
Xu, Y., Moseley, J. B., Sagot i Poy, F., Pellman, D., Goode, B. L. and Eck, M. J. (2004). Crystal structures of a Formin Homology-2 domain reveal a tethered dimer architecture. *Cell* **116**, 711-723.
Zigmond, S. H., Evangelista, M., Boone, C., Yang, C., Dar, A. C., Sicheri, F., Forkey, J. and Pring, M. (2003). Formin leaky cap allows elongation in the presence of tight capping proteins. *Curr. Biol.* **13**, 1820-1823.